

LETTER • OPEN ACCESS

Quantifying the contribution of major carbon producers to increases in vapor pressure deficit and burned area in western US and southwestern Canadian forests

To cite this article: Kristina A Dahl *et al* 2023 *Environ. Res. Lett.* **18** 064011

View the [article online](#) for updates and enhancements.

You may also like

- [High-severity fire: evaluating its key drivers and mapping its probability across western US forests](#)
Sean A Parks, Lisa M Holsinger, Matthew H Panunto *et al.*
- [Wildfire activity is driving summertime air quality degradation across the western US: a model-based attribution to smoke source regions](#)
Taylor Y Wilmot, Derek V Mallia, A Gannet Hallar *et al.*
- [How will climate change affect wildland fire severity in the western US?](#)
Sean A Parks, Carol Miller, John T Abatzoglou *et al.*

UNITED THROUGH SCIENCE & TECHNOLOGY



The Electrochemical Society
Advancing solid state & electrochemical science & technology

248th ECS Meeting Chicago, IL October 12-16, 2025 *Hilton Chicago*



Science + Technology + YOU!

SUBMIT ABSTRACTS by March 28, 2025

[SUBMIT NOW](#)

ENVIRONMENTAL RESEARCH
LETTERS

LETTER

OPEN ACCESS

RECEIVED
14 October 2022REVISED
5 February 2023ACCEPTED FOR PUBLICATION
17 February 2023PUBLISHED
16 May 2023

Original content from
this work may be used
under the terms of the
[Creative Commons
Attribution 4.0 licence](#).

Any further distribution
of this work must
maintain attribution to
the author(s) and the title
of the work, journal
citation and DOI.

Quantifying the contribution of major carbon producers to
increases in vapor pressure deficit and burned area in western US
and southwestern Canadian forestsKristina A Dahl^{1,*} , John T Abatzoglou² , Carly A Phillips³ , J Pablo Ortiz-Partida¹ , Rachel Licker⁴ ,
L Delta Merner⁴ and Brenda Ekwurzel⁴ ¹ Climate & Energy Program, Union of Concerned Scientists, Oakland, CA, United States of America² Management of Complex Systems Department, University of California, Merced, CA, United States of America³ Climate & Energy Program, Union of Concerned Scientists, Cambridge, MA, United States of America⁴ Climate & Energy Program, Union of Concerned Scientists, Washington, DC, United States of America

* Author to whom any correspondence should be addressed.

E-mail: kdahl@ucsusa.org**Keywords:** wildfire, attribution, fossil fuels, climate impacts, droughtSupplementary material for this article is available [online](#)

Abstract

Increases in burned forest area across the western United States and southwestern Canada over the last several decades have been partially driven by a rise in vapor pressure deficit (VPD), a measure of the atmosphere's drying power that is significantly influenced by human-caused climate change. Previous research has quantified the contribution of carbon emissions traced back to a set of 88 major fossil fuel producers and cement manufacturers to historical global mean temperature rise. In this study, we extend that research into the domain of forest fires. We use a global energy balance carbon-cycle model, a suite of climate models, and a burned area (BA) model to determine the contribution of emissions traced to the major carbon producers to the long-term increase in VPD during 1901–2021 and to cumulative forest fire area during 1986–2021 in the western US and southwestern Canada. Based on climate model data, we find that emissions traced to these carbon producers contributed 48% (interquartile range (IQR) 38%–63%) of the long-term rise in VPD between 1901 and 2021. BA modeling indicates that these emissions also contributed 37% (IQR 26%–47%) of the cumulative area burned by forest fires between 1986 and 2021 in the western US and southwestern Canada. The increase in VPD in this region is linked to both increased fire activity and the region's current and prolonged megadrought. As loss and damage from these hazards mounts, this research can inform public and legal dialogues regarding the responsibility carbon producers bear for addressing past, present, and future climate risks associated with fires and drought in the western US and southwestern Canada.

1. Introduction

Over the last several decades, the western United States and southwestern Canada have experienced increases in the area burned by wildfires (Abatzoglou and Williams 2016, Hanes *et al* 2019, Balch *et al* 2022), the number of large fires (Dennison *et al* 2014, Westerling 2016), the length of the fire season (Westerling 2016, Kirchmeier-Young *et al* 2017, Goss *et al* 2020), the elevation at which fires burn (Alizadeh *et al* 2021), and the extent of forested lands that burn at high severity (Parks and Abatzoglou 2020). These

trends, particularly evident in the region's forested ecosystems, coincide with a twofold increase in Canadian fire suppression costs and a more than sevenfold increase in US federal suppression costs when comparing average costs from 1985–1989 to those of 2013–2017 (Canada; Natural Resources Canada 2021) or 2017–2021 (US; National Interagency Fire Center 2022).

Significant portions of many of these trends in wildfire activity have been attributed to anthropogenic climate change (Abatzoglou and Williams 2016, Kirchmeier-Young *et al* 2017, Williams *et al* 2019,

Zhuang *et al* 2021). Vapor pressure deficit (VPD)—a measure of atmospheric water demand defined as the difference between the amount of water vapor in the air and the amount of water vapor that air would hold at saturation—has emerged as a key metric linking climate change and burned area (BA) due to its role in regulating ecosystem water dynamics (Grossiord *et al* 2020, Clarke *et al* 2022). Through the lens of regional wildfire risk, rising VPD ultimately translates to a greater likelihood that fuels will ignite and carry fire across a landscape.

More than two-thirds of the observed summertime increase in VPD in the western US has been attributed to anthropogenic warming (Zhuang *et al* 2021). In turn, the increase in summertime VPD has driven increases in fuel aridity in the region, resulting in nearly a doubling of BA in western US forests during 1984–2015 (Abatzoglou and Williams 2016). Regionally, there is a strong and established interannual relationship between VPD and BA across forested subregions of the western US and southwestern Canada (Abatzoglou *et al* 2018, Williams *et al* 2019, Whitman *et al* 2022). In flammability-limited ecosystems like forests, area burned is exponentially related to VPD (Juang *et al* 2022).

The question of who bears responsibility for climate change and impacts such as increases in BA is being actively explored in both scientific and legal realms. The current global governance system to address climate change is centered on the responsibilities of nation states, but corporate actors also bear a distinct responsibility for the climate crisis. Recent research has found that carbon dioxide and methane emissions traced to major fossil fuel and cement manufacturing companies have contributed to more than 40% of rising global temperatures, 25% of global sea level rise, and 50% of ocean acidification between 1880 and the 2010s (Ekwurzel *et al* 2017, Licker *et al* 2019). However, their role in setting the stage for the increased fire extent observed in the western US and southwestern Canada in recent decades has gone unexamined.

This study establishes the role of major carbon producers in increasing wildfire risks in forested landscapes by examining two primary research questions: (a) what is the quantifiable relationship between changes in VPD in western North America and changes in global mean temperature (GMT)? and (b) given a quantified relationship between GMT and VPD, how much have emissions from major carbon producers contributed to the observed increase in VPD and the cumulative forest BA in the western United States and southwestern Canada? By addressing these questions, this study advances the source attribution literature as well as national and international dialogues around liability for climate impacts.

2. Methods

2.1. Observed and modeled VPD data

Observed monthly maximum temperature, minimum temperature, and vapor pressure for North America at a $\frac{1}{4}$ degree horizontal resolution during 1901–2021 was acquired from Williams *et al* (2022). We calculated monthly mean VPD at the native pixel scale by first calculating saturation vapor pressure from monthly average maximum and minimum temperature and having VPD set as the difference between actual and saturation vapor pressure following Seager *et al* 2015.

Monthly maximum temperature, minimum temperature, and specific humidity data from 28 coupled model intercomparison project, phase 6 (CMIP6) climate models were acquired for both the historical (1850–2014) and SSP2-4.5 (2015–2100) experiments (table S1) and interpolated to a common 1.0-degree horizontal resolution grid before calculating VPD as above. We then calculated the change in VPD over time by multiplying the linear least squares trend by the number of years in the time period of interest. Unless otherwise specified, throughout this study we used the same linear least squares approach to calculate the change in all modeled and observed climate variables over time.

2.2. Establishing a GMT-VPD relationship

We constrained our analysis to forested lands based on level III U.S. Environmental Protection Agency (EPA) ecoregions of the western United States and southwestern Canada in the area west of 103°W and between 30° and 53°N. We focused on March–September mean VPD over forested areas of this domain given the influence of antecedent and concurrent VPD in curing fuels and making them receptive to igniting and carrying fire (e.g. Abatzoglou *et al* 2013, Jolly *et al* 2015) as evident in strong relationships between seasonal aggregates of VPD and macroscale BA in the region (e.g. Abatzoglou *et al* 2021).

To evaluate relationships between the change in GMT and the change in March–September VPD averaged across the study area in both observations and climate models, we acquired observed GMT from NASA-GISS from 1880–2021 (Hansen *et al* 2010) and modeled GMT for each unique CMIP6 climate model and ensemble member. We calculated the rate of change in regional March–September VPD per degree change in GMT as the difference in VPD and GMT between 1991–2020 and 1901–1950 (equation (1)),

$$\frac{\Delta \text{VPD}}{\Delta \text{GMT}} = \frac{\text{VPD}_{1991-2020} - \text{VPD}_{1901-1950}}{\text{GMT}_{1991-2020} - \text{GMT}_{1901-1950}}. \quad (1)$$

2.2.1. Assessing the influence of internal variability

Internal multidecadal variability has influenced the observed trajectory of climate, including the

aridification across the study domain during the past half century (Abatzoglou and Williams 2016, Zhuang *et al* 2021). By averaging over multidecadal time periods and focusing on changes over a 120 year period in equation (1), we aim to minimize the influence of internal variability on estimates of $\Delta\text{VPD}/\Delta\text{GMT}$. We assessed the degree to which internal variability could influence the relationship between regional VPD and GMT by calculating $\Delta\text{VPD}/\Delta\text{GMT}$ for time periods of at least 50 years in length for model years 1901–2020. We then calculated the linear least squares trends in VPD and GMT for each time period and examined the ratio of the two. This was done in a combinatorial fashion that included incrementing the length of time periods by 10 years (e.g. 50 years, 60 years) for each model and staggering the initial year for each trend calculation by 10 years (e.g. 1901, 1911).

2.2.2. Assessing linear scaling

Our methodology assumes that changes in VPD scale linearly with changes in GMT. The scientific literature suggests that many local changes in climate scale linearly with changes in GMT (Mitchell 2003). Pattern scaling has been widely used both because of its simplicity and because the assumption of linear relationships generally holds well for thermal variables and climate summaries such as seasonal values (James *et al* 2017, Lee *et al* 2021). Since VPD is directly related to local temperature changes by construction of the saturation vapor pressure, and relative humidity is projected to decline slightly over land with anthropogenic warming, we expected VPD to reasonably adhere to linear scaling.

We assessed the validity of linear VPD-GMT relationships by calculating the R^2 value between trajectories in the 21 year centered moving average VPD versus the 21 year centered change in GMT and the linear least squares fit of the data for each model.

2.3. Determining the GMT contribution of the largest carbon producers

After establishing $\Delta\text{VPD}/\Delta\text{GMT}$, we simulated changes in GMT using an energy balance carbon cycle climate model so that the $\Delta\text{VPD}/\Delta\text{GMT}$ relationship could be applied to the output. The model is based on (Millar *et al* 2017) with parameters defined by Ekwurzel *et al* (2017).

We first ran a ‘full forcing’ (i.e. including volcanic eruptions, solar activity, total fossil fuel emissions, etc) GMT simulation with energy balance and carbon cycle parameters that provided the best fit to observed changes in atmospheric CO_2 and GMT since 1750 (see Licker *et al* 2019, supplementary tables 1 and 2). We then ran the model again with the scope 1 and scope 3 carbon dioxide and methane emissions of the world’s 88 largest carbon producers

(hereafter ‘the big 88’) removed between 1900 and 2015 using annual, producer-specific emissions data (Licker *et al* 2019 table 7, Climate Accountability Institute 2020). This enabled us to calculate the annual GMT change resulting from emissions traced to the big 88, $\Delta\text{GMT}_{\text{big88}}(t)$. We refer to this as the ‘X88’ simulation.

Annual emissions data from the big 88 is not uniformly available for the post-2015 period—a period of significant wildfire activity in the study region. Rather than simulating $\Delta\text{GMT}_{\text{big88}}$ for 2016–2021, we hold $\Delta\text{GMT}_{\text{big88}}(t)$. Two lines of evidence suggest this approach will yield conservative results. First, annual emissions data for a subset of the big 88 between 2015 and 2018 show that each entity’s emissions increased every year through 2018 (figures S2 and S3). Second, average annual global CO_2 emissions from fossil fuel and industry were higher over the 2016–2021 period than in 2015 (Friedlingstein *et al* 2021, Liu *et al* 2022). Results for the full 1900–2021 period are reported here. Results for the 1901–2015 period are reported in table S2.

Consistent with previous studies, we also ran the energy balance carbon cycle climate model with and without total fossil fuel aerosols for both the full forcing and the X88 cases (Licker *et al* 2019). Since the big 88 contribute roughly two-thirds of the total industrial aerosol emissions, however, excluding the aerosols underestimates the net cooling influence of that forcing. We therefore focus on the best estimate with full forcing, including total fossil fuel aerosols.

The order of removal of each of the 88 carbon producers within the model has a potential, albeit slight, influence on its respective contribution to GMT. To assess this source of uncertainty, for each carbon producer, we first ran the model with only that producer’s emissions, i.e. without the emissions of the remaining 87. We then ran the model again assuming that the producer’s emissions were added last in the set of 88.

We then determined the simulated difference in annual GMT between the full forcing and X88 simulation results. These annual $\Delta\text{GMT}_{\text{big88}}$ findings were then incorporated into VPD and BA time series based on the 28 CMIP6 climate models and observational data.

2.4. VPD and BA contributions

Forested BA data were acquired from three datasets: (a) Monitoring Trends in Burn Severity in the western US from 1984–2020 (Eidenshink *et al* 2007); (b) Canadian National Burned Area Composite in Canada from 1986–2020 (Hall *et al* 2020); and (c) MODIS BA (MCD64A1) from 2001–2021 (Giglio *et al* 2018). The latter was used to estimate BA for 2021 based on a linear model between BA from MODIS and each of the respective datasets during periods of overlap following Williams *et al* 2014. We limited our analysis to BA in the western US and southwestern

Canada within forested level III ecoregions to match the geographic extent of the VPD data.

To calculate the portion of the VPD change from 1901–2021 resulting from emissions traced to the big 88, we constructed counterfactual VPD time series for the observational data set and for each CMIP6 model. The counterfactuals represent VPD change without the influence of the big 88 and were developed by multiplying the annual $\Delta\text{GMT}_{\text{big88}}$ for each year by the $\Delta\text{VPD}/\Delta\text{GMT}$ identified previously for each dataset. The VPD change contributed by the big 88 was calculated as the difference between the total modeled or observed VPD change and the counterfactual (equation (2)),

$$\text{VPD}_c(t) = \text{VPD}_m(t) - (\Delta\text{VPD}/\Delta\text{GMT})_m \cdot \Delta\text{GMT}_{\text{big88}}(t) \quad (2)$$

where t represents year, and VPD_c represents the counterfactual VPD for each model, m .

Following Abatzoglou and Williams (2016), we considered counterfactual BA scenarios that exclude the modeled influence of the big 88 from the observed VPD record. Because reliable BA observations are only available starting in the mid-1980s, our counterfactual BA analysis covers the 1986–2021 period. Model results indicated that the influence of the big 88's emissions grew substantially between 1901 and 1986. To avoid devaluing the importance of the big 88's emissions in shaping climate before 1986, we report VPD contributions since both 1901 and 1986, and BA contributions since 1986.

To calculate the counterfactual BA, we used a simple macroscale empirical model of annual forest BA of the form:

$$\log(\text{BA}(t)) = \alpha + \beta \cdot \text{VPD}(t) + \varepsilon \quad (3)$$

where t is the year, α and β are regression coefficients, and ε represents an error term (Abatzoglou *et al* 2021). This modeling exercise is based on the strong exponential VPD-BA relationship in the observational record (Juang *et al* 2022). The error term is drawn from residuals in the aforementioned equation when omitting ε and is meant to capture stochasticity in relationships not captured in VPD (e.g. fire weather conditions, human ignitions).

As above, counterfactual VPD time series excluding the influence of the big 88 and the time varying influence of the big 88 on GMT were constructed based on the observed VPD time series following equation (4):

$$\text{VPD}_{c,\text{obs}}(t) = \text{VPD}_{\text{obs}} - (\Delta\text{VPD}/\Delta\text{GMT})_m \cdot \Delta\text{GMT}_{\text{big88}}(t). \quad (4)$$

This approach removes the time varying increase in GMT resulting from emissions traced to the big 88, leaving much of the interannual variability from the observed record unchanged. We then applied the

counterfactual VPD time series ($\text{VPD}_{c,\text{obs}}$) for each model to equation (3) to estimate BA during 1986–2021 in the absence of carbon emissions from the big 88. Following previous work, we use counterfactuals from observations to best adhere with realized BA (Abatzoglou and Williams 2016). We ran each counterfactual model 100 times for each climate model to account for randomized time series of ε in modeled BA and present results for the median of each of the 28 CMIP6 models. The cumulative forest BA resulting from emissions traced to the big 88 was calculated by taking the difference between cumulative observed forest BA and cumulative forest BA simulated using the counterfactual VPD time series. We assessed the validity of this modeling approach by comparing modeled cumulative BA using equation (3) and the observed VPD time series data that include the influence of the big 88 (running the model 100 times to account for random ε terms) to the observed forest BA.

3. Results

3.1. Relationship between GMT and regional VPD

Observed regional March–September VPD as calculated by linear least squares regression increased by 0.82 hPa from 1901–2021, consistent with findings from previous studies (e.g. Williams *et al* 2022). This represents an 11.2% increase in VPD over the study period. We also note that 21 of the 22 years since 2000 have had March–September VPD above the 1901–1950 average. All CMIP6 models captured the historical increase in VPD, with a 28-model mean increase of 0.80 hPa (interquartile range (IQR) 0.53–1.03 hPa) over the same time period (figure 1(a)).

The observational data showed a positive relationship between GMT and regional March–September VPD of 0.99 hPa °C^{−1} or 13.4% °C^{−1}. All CMIP6 models also showed a positive relationship between GMT and regional March–September VPD, with a 28-model mean of 0.81 hPa °C^{−1} (IQR 0.53 hPa °C^{−1}–1.05 hPa °C^{−1}) or 12.9% °C^{−1} (figures 1(b) and (c)). The spread in $\Delta\text{VPD}/\Delta\text{GMT}$ within the model suite likely reflects the combination of internal variability within each model and inter-model differences in physics. Estimates of the influence of internal variability on $\Delta\text{VPD}/\Delta\text{GMT}$ for each model (figure S1), however, suggest that uncertainty in $\Delta\text{VPD}/\Delta\text{GMT}$ from inter-model differences exceeds that from internal variability, similar to results from studies that have examined sources of uncertainty for regional temperature change (Hawkins and Sutton 2009).

The relationship between 21 year moving average changes in regional VPD and 21 year moving averages in GMT are quasi-linear from the mid-20th century onwards (figure 1(b)), suggestive of a scalable, albeit model dependent, GMT-regional VPD relationship. Linear scaling of $\Delta\text{VPD}/\Delta\text{GMT}$ is further

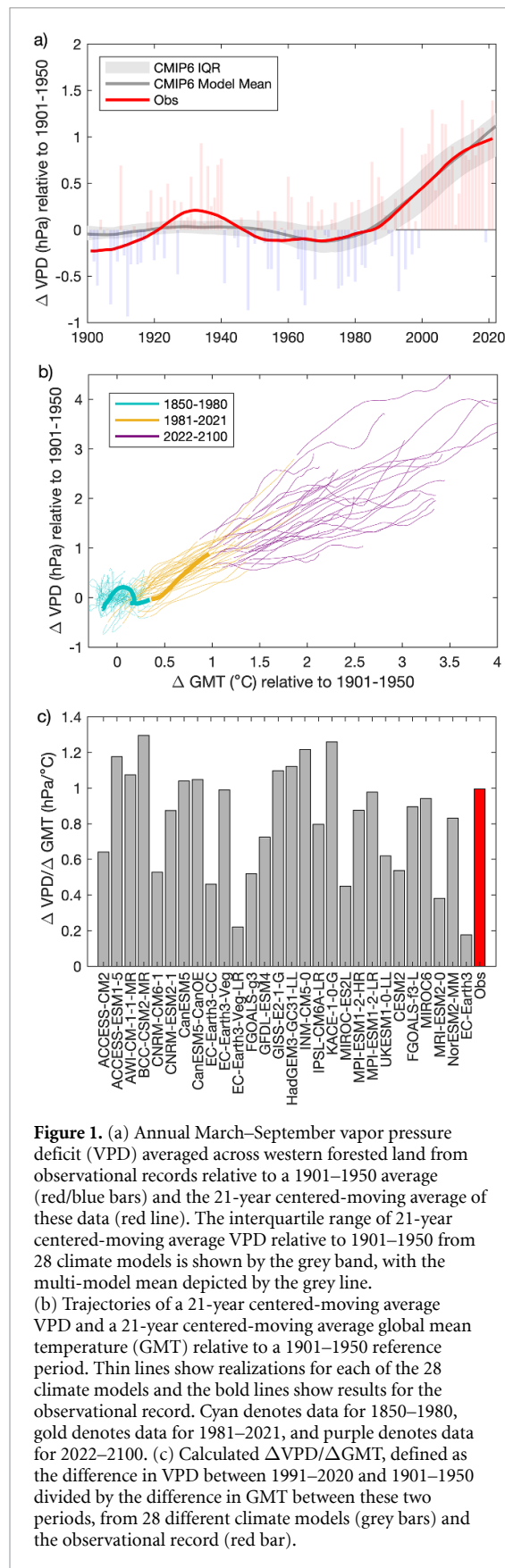


Figure 1. (a) Annual March–September vapor pressure deficit (VPD) averaged across western forested land from observational records relative to a 1901–1950 average (red/blue bars) and the 21-year centered-moving average of these data (red line). The interquartile range of 21-year centered-moving average VPD relative to 1901–1950 from 28 climate models is shown by the grey band, with the multi-model mean depicted by the grey line. (b) Trajectories of a 21-year centered-moving average VPD and a 21-year centered-moving average global mean temperature (GMT) relative to a 1901–1950 reference period. Thin lines show realizations for each of the 28 climate models and the bold lines show results for the observational record. Cyan denotes data for 1850–1980, gold denotes data for 1981–2021, and purple denotes data for 2022–2100. (c) Calculated $\Delta\text{VPD}/\Delta\text{GMT}$, defined as the difference in VPD between 1991–2020 and 1901–1950 divided by the difference in GMT between these two periods, from 28 different climate models (grey bars) and the observational record (red bar).

confirmed by noting that 22 of the 28 models had $R^2 > 0.75$ (all models had $R^2 > 0.5$) for a linear relationship between 21-year moving average regional VPD and GMT during the 1901–2020 period. These

results suggest that linear scaling adequately captures the $\Delta\text{VPD}/\Delta\text{GMT}$ response.

The period from 1986–2021, for which reliable BA data is available for the region, is characterized by steep, steady rise in VPD. As calculated by linear least squares regression over 1986–2021, March–September VPD increased by 1.09 hPa in the observational data and by 1.13 hPa (IQR 0.71–1.43 hPa) in the 28-model mean over that time period.

3.2. Contribution of the big 88 to GMT and regional VPD

Consistent with the results of Ekwurzel *et al* (2017), we find that the influence of the big 88 on GMT grows over time. In the early years of the 20th century, $\Delta\text{GMT}_{\text{big88}}(t)$ is nearly negligible. However, $\Delta\text{GMT}_{\text{big88}}(t)$ increases exponentially to 0.49°C by 2021. The best-estimate climate model accounts for $49.1\% \pm 1.3\%$ of the observed warming between 1900 and 2015 in our X88 simulation.

Applying the established $\Delta\text{VPD}/\Delta\text{GMT}$ relationship, the total contribution of emissions from the big 88 to VPD change for the 1901–2021 period is 0.47 hPa per the observational data, or 57% of total observed change in VPD. The total contribution of the big 88's emissions to VPD change per the 28-model mean is slightly lower at 0.39 hPa (IQR 0.25–0.50), or 48% (IQR 32%–63%) of the total modeled VPD change over the study period (figure 2). The models and observations thus imply that roughly half of the increase in VPD from 1901–2021 can be traced to the emissions of these major carbon producers.

Over the 1986–2021 time period, the total contribution of emissions from the big 88 to VPD is 0.33 hPa in the observational data and 0.27 hPa (IQR 0.18–0.35 hPa) for the 28-model mean. Given this shorter time period, these results may be more prone to the influence of internal variability within the models than results from the full 1901–2021 time period.

3.3. Contribution of the big 88 to BA in forested lands

As in previous studies, forest BA grows exponentially with increased VPD (figure 3). Using VPD time series that do not exclude the influence of the big 88, we approximate modeled cumulative BA of 217 100 km², which is comparable to the observed cumulative BA of 214 690 km². The differences between observed and modeled BA were not statistically significant.

We modeled BA that excluded the influence of the big 88 for each of the 28 CMIP6 models using a counterfactual VPD time series that removes the model dependent $\Delta\text{VPD}/\Delta\text{GMT}$ from the observed VPD data. Without emissions traced back to the big 88, we find that a central estimate of cumulative BA in the region would have been 134 735 km² (IQR 112 000–156 000 km²). We thus conclude that emissions from the big 88 contributed 37% (IQR 26%–47%) of

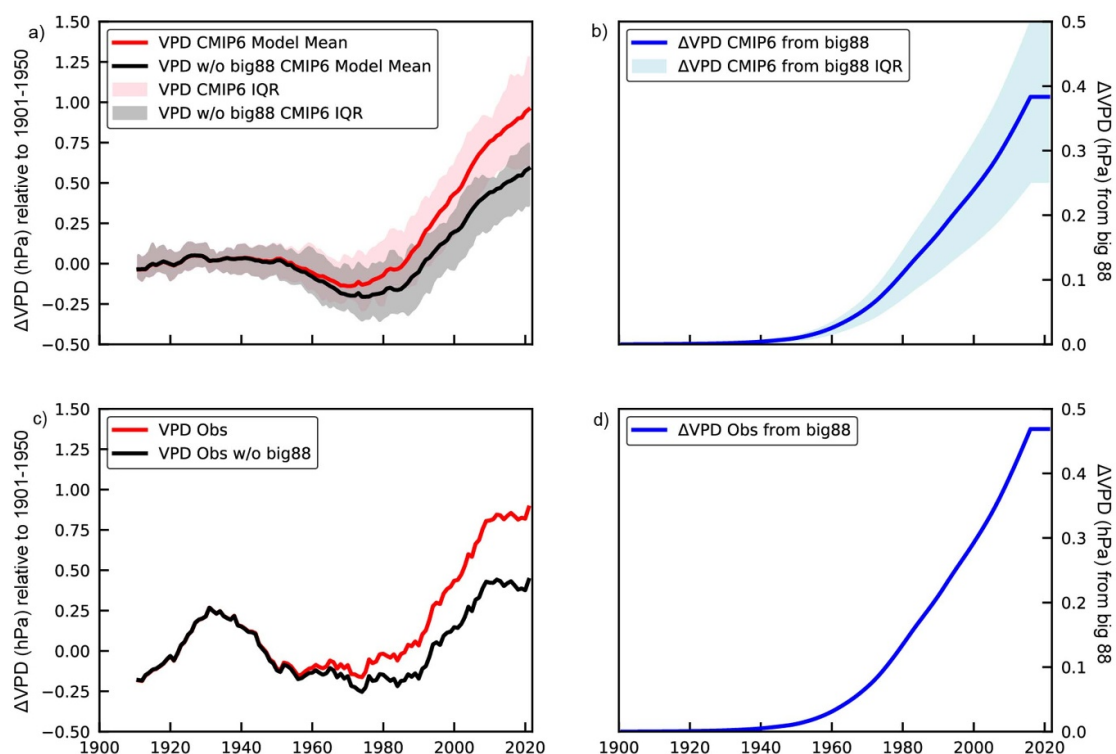


Figure 2. (a) Multi-model mean (red line) and interquartile range (pink shading) of regional March–September vapor pressure deficit (VPD) based on 28 climate models relative to the 1901–1950 average. Black line and gray shading show the multi-model mean and interquartile range of the counterfactual VPD change without the influence of emissions traced to 88 major carbon producers. Data are shown as a 21-year moving average. (b) Multi-model mean (blue line) and interquartile range (blue shading) of the change in VPD resulting from emissions from the 88 major carbon producers. (c) and (d) As for (a) and (b), but for observational data.

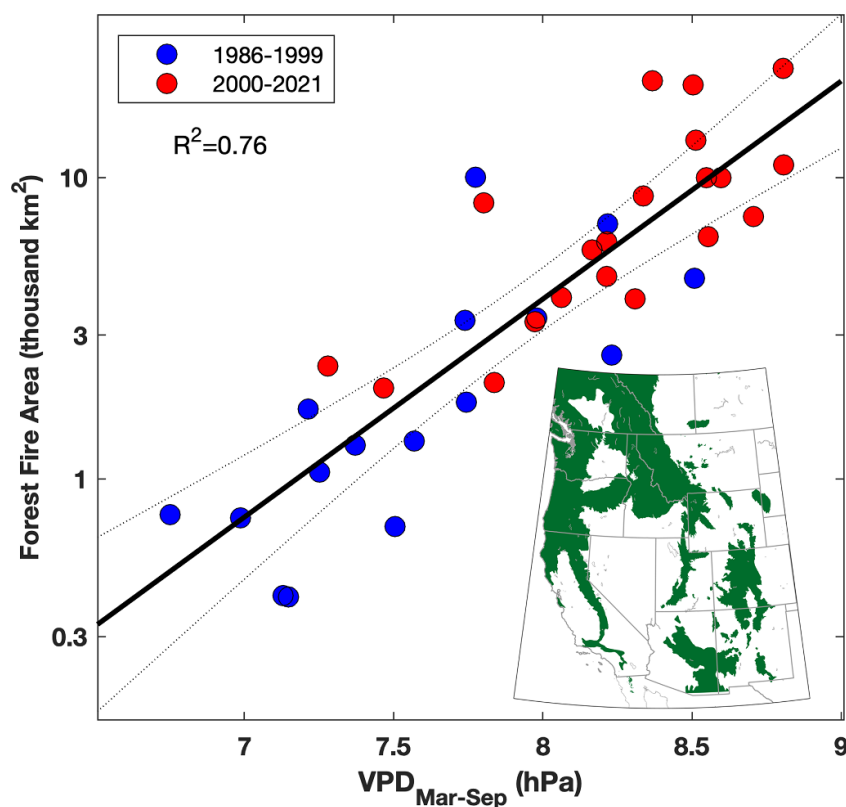
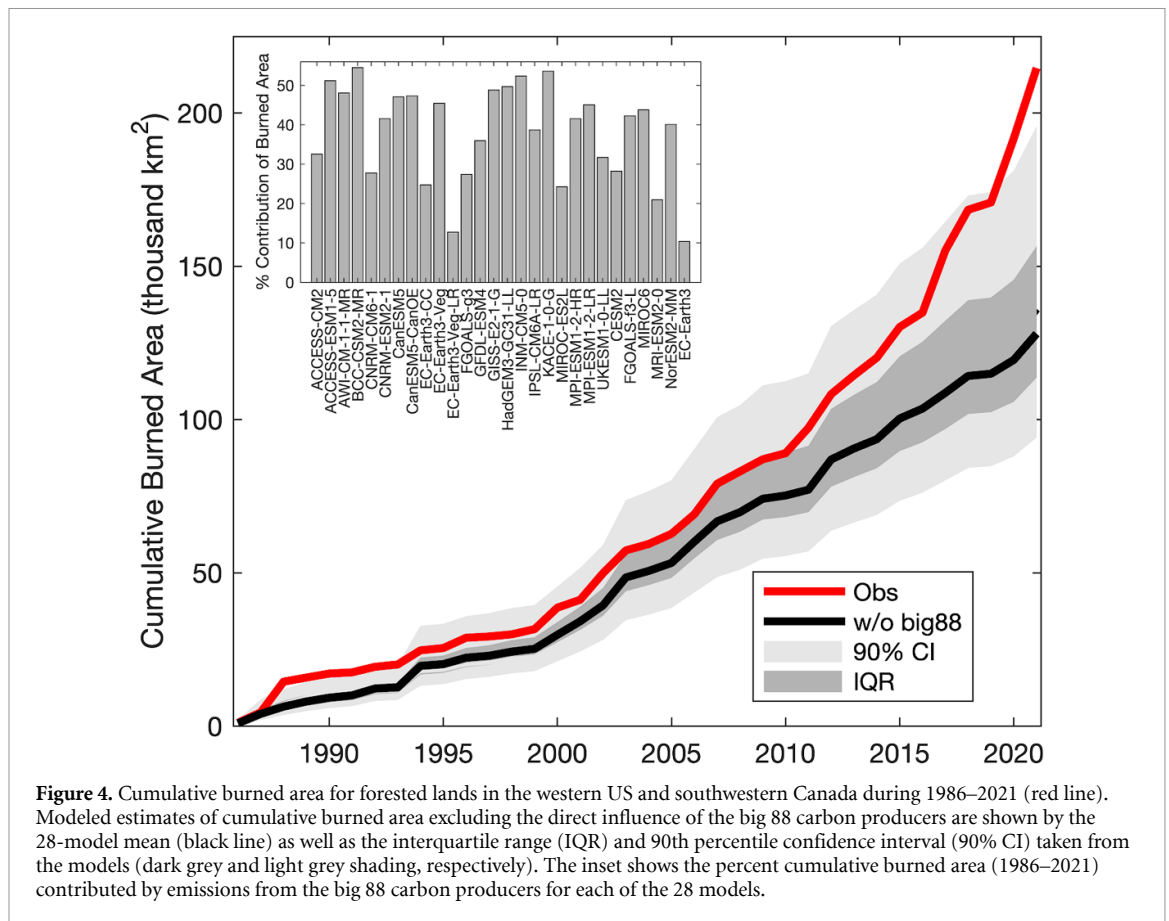


Figure 3. Scatterplot of March–September vapor pressure deficit (VPD) versus the base-10 logarithm of burned area in forested ecoregions (area highlighted green in the inset box) during 1986–2021. Data for years 1986–1999 are shown in blue, data for years 2000–2021 are shown in red, and the solid and dashed lines show the regression ($p < 0.000\ 01$) and its 95th percentile confidence interval, respectively.



the cumulative burned forest area from 1986–2021 (figure 4). This represents roughly 80 000 km² (nearly 20 million acres) of burned forest area, or an area larger than Ireland.

4. Discussion and conclusion

Ecosystems, communities, and individuals in the western US and southwestern Canada are already being affected by increases in temperature and VPD. Such changes have catalyzed an increase in wildfire (Westerling *et al* 2006) and other forest disturbances across the region (Anderegg *et al* 2022). The rapid release of greenhouse gases during forest fires and the transition to non-forest ecosystem types following large, high-severity forest fires also serve to exacerbate climatic warming (Stevens-Rumann *et al* 2018).

Community-level impacts have been profound. Wildfires in California between 2017 and 2022 killed 194 people (CalFire 2022). The state's 2018 fire season alone resulted in the destruction of more than 22 000 structures (CalFire 2018) and damages exceeding \$140 billion (Wang *et al* 2021). Fire suppression costs across the United States exceeded \$3 billion that same year (National Interagency Fire Center 2022). In addition to direct threats to lives and property, wildfires can reduce air quality and produce particulate matter that affects human and public health in many ways (Haikerwal *et al* 2016, Chen *et al* 2021, Heft-Neal

et al 2022). Low-income families disproportionately experience these risks (Burke *et al* 2022).

As the regional climate has warmed and VPD has increased over the last several decades, atmospheric evaporative demand has risen (Albano *et al* 2022). The consequences of this high atmospheric 'thirst' over the course of seasons or years extend beyond fire and its impacts and include drought, greater evapotranspiration, vegetation drying, and reduced streamflow (Albano *et al* 2022).

These consequences are currently being experienced across western North America amidst the current 22-year-long megadrought (Williams *et al* 2022). In 2020 alone, a combination of low precipitation and high temperature and VPD reduced gross primary production across the western United States by more than 25% (Dannenberg *et al* 2022). In California, the direct costs of drought for agriculture during 2021–2022 were estimated at \$3.0 billion and nearly 22 000 lost jobs (Medellín-Azuara *et al* 2022). Moreover, people in rural, disadvantaged communities have lost water access or experienced water contamination due to groundwater overextraction (Perrone and Jasechko 2017, Stokstad 2020). These impacts have led to additional costs, including \$500 million in drought assistance programs (DWR 2021).

Our results highlight the roles of major carbon producers in driving forest fire extent by enhancing fuel aridity, but do not explicitly account for effects

from non-climatic factors such as the prohibition of Indigenous burning, legacies of fire suppression, or changing human ignitions. At the stand and landscape level, these factors have contributed to changes in forest characteristics in the region (Scholl and Taylor 2010, Collins *et al* 2011, Hagmann *et al* 2021). While such changes play a critical role in driving the size and severity of individual fires across the region, they have not modified the climate-BA relationship at the scale of this study (Williams *et al* 2019).

With the impacts of climate change growing increasingly severe, questions of who is responsible for climate change, how much responsibility each entity bears, and the obligations of those entities to mitigate future climate change and assist financially with climate adaptation are more present than ever in policy negotiations and in courtrooms around the world. These questions are deepened by the fact that the fossil fuel industry was aware of the climate-related risks of their products as early as the mid-1960s (Franta 2018) and, instead of shifting business practices, invested in campaigns and tactics to mislead the public and generate doubt about climate science (Supran and Oreskes 2017, 2021, Franta 2018).

Here, we find that the emissions of the world's largest 88 carbon producers contributed 48% of the increase in VPD since 1901 and 37% of the cumulative BA in the forested lands of western US and southwestern Canada since 1986, establishing the regional impacts of climate change in relation to corporate emitters and underscoring the responsibility these companies bear for the impacts of climate change. These impacts extend far beyond a given fire scar and cause both direct and indirect harm to economies, ecosystems, public health, and communities. As noted in the latest UN Intergovernmental Panel on Climate Change assessment (IPCC 2022), climate governance and adaptation cannot exist exclusively at the level of nation-states, which necessitates quantitative research connecting impacts to emissions sources. This study adds to a growing body of research that can inform public, policy, and legal discussions regarding the responsibility of carbon producers for past, present and future climate risks.

Data availability statement

The data that support the findings of this study are openly available at the following URL/DOI: [10.7910/DVN/VRLTG5](https://doi.org/10.7910/DVN/VRLTG5).

Acknowledgments

The authors thank two anonymous reviewers for careful reviews that improved this manuscript. This research was made possible by the generous support of the Barr Foundation, Blanchette Hooker Rockefeller Fund, Farvue Foundation, Foundation for International Law for the Environment, Grantham

Foundation for the Protection of the Environment, MacArthur Foundation, Rockefeller Family Fund, Scherman Foundation, Wallace Global Fund, Water Foundation, individual donors, and members of the Union of Concerned Scientists.

Conflict of interest

The authors report no conflicts of interest.

ORCID iDs

Kristina A Dahl  <https://orcid.org/0000-0001-6471-8845>
 John T Abatzoglou  <https://orcid.org/0000-0001-7599-9750>
 Carly A Phillips  <https://orcid.org/0000-0003-1232-2683>
 J Pablo Ortiz-Partida  <https://orcid.org/0000-0001-9688-2607>
 Rachel Licker  <https://orcid.org/0000-0001-7191-0691>
 L Delta Merner  <https://orcid.org/0009-0006-1217-312X>
 Brenda Ekwurzel  <https://orcid.org/0000-0003-3950-281X>

References

- Abatzoglou J T, Battisti D S, Williams A P, Hansen W D, Harvey B J and Kolden C A 2021 Projected increases in western US forest fire despite growing fuel constraints *Commun. Earth Environ.* **2** 1–8
- Abatzoglou J T, Kolden C A, Abatzoglou J T and Kolden C A 2013 Relationships between climate and macroscale area burned in the western United States *Int. J. Wildland Fire* **22** 1003–20
- Abatzoglou J T and Williams A P 2016 Impact of anthropogenic climate change on wildfire across western US forests *Proc. Natl Acad. Sci. USA* **113** 11770–5
- Abatzoglou J T, Williams A P, Boschetti L, Zubkova M and Kolden C A 2018 Global patterns of interannual climate–fire relationships *Glob. Change Biol.* **24** 5164–75
- Albano C M, Abatzoglou J T, McEvoy D J, Huntington J L, Morton C G, Dettinger M D and Ott T J 2022 A multidataset assessment of climatic drivers and uncertainties of recent trends in evaporative demand across the continental United States *J. Hydrometeorol.* **23** 505–19
- Alizadeh M R, Abatzoglou J T, Luce C H, Adamowski J F, Farid A and Sadegh M 2021 Warming enabled upslope advance in western US forest fires *Proc. Natl Acad. Sci.* **118** e2009717118
- Anderegg W R L, Chegwidden O S, Badgley G, Trugman A T, Cullenward D, Abatzoglou J T, Hicke J A, Freeman J and Hamman J J 2022 Future climate risks from stress, insects and fire across US forests *Ecol. Lett.* **25** 1510–20
- Balch J K, Abatzoglou J T, Joseph M B, Koontz M J, Mahood A L, McGlinchy J, Cattau M E and Williams A P 2022 Warming weakens the night-time barrier to global fire *Nature* **602** 442–8
- Burke M *et al* 2022 Exposures and behavioural responses to wildfire smoke *Nat. Hum. Behav.* **6** 1–11
- CalFire 2018 *Wildfire Activity Statistics* (Sacramento, CA) (available at: www.fire.ca.gov/media/330lgmwb/2018_redbook_final.pdf)
- CalFire 2022 Stats & Events (available at: www.fire.ca.gov/stats-events/)

- Chen G *et al* 2021 Mortality risk attributable to wildfire-related PM_{2.5} pollution: a global time series study in 749 locations *Lancet Planet. Health* **5** e579–87
- Clarke H, Nolan R H, De Dios V R, Bradstock R, Griebel A, Khanal S and Boer M M 2022 Forest fire threatens global carbon sinks and population centres under rising atmospheric water demand *Nat. Commun.* **13** 7161
- Climate Accountability Institute 2020 Carbon majors 2018 data set (available at: https://climateaccountability.org/carbonmajors_dataset2020.html)
- Collins B M, Everett R G and Stephens S L 2011 Impacts of fire exclusion and recent managed fire on forest structure in old growth Sierra Nevada mixed-conifer forests *Ecosphere* **2** art51
- Dannenberg M P *et al* 2022 Exceptional heat and atmospheric dryness amplified losses of primary production during the 2020 U.S. Southwest hot drought *Glob. Change Biol.* **28** 4794–806
- Dennison P E, Brewer S C, Arnold J D and Moritz M A 2014 Large wildfire trends in the western United States, 1984–2011 *Geophys. Res. Lett.* **41** 2928–33
- DWR 2021 Drought Funding *California Department of Water Resources* (available at: <https://water.ca.gov/Water-Basics/Drought/Drought-Funding>)
- Eidenshink J, Schwind B, Brewer K, Zhu Z-L, Quayle B and Howard S 2007 A project for monitoring trends in burn severity *Fire Ecol.* **3** 3–21
- Ekwurzel B, Boneham J, Dalton M W, Heede R, Mera R J, Allen M R and Frumhoff P C 2017 The rise in global atmospheric CO₂, surface temperature, and sea level from emissions traced to major carbon producers *Clim. Change* **144** 579–90
- Franta B 2018 Early oil industry knowledge of CO₂ and global warming *Nat. Clim. Change* **8** 1024–5
- Friedlingstein P *et al* 2021 Global carbon budget 2020 *Earth Syst. Sci. Data* **12** 3269–340
- Giglio L, Boschetti L, Roy D P, Humber M L and Justice C O 2018 The collection 6 MODIS burned area mapping algorithm and product *Remote Sens. Environ.* **217** 72–85
- Goss M, Swain D L, Abatzoglou J T, Sarhadi A, Kolden C A, Williams A P and Diffenbaugh N S 2020 Climate change is increasing the likelihood of extreme autumn wildfire conditions across California *Environ. Res. Lett.* **15** 094016
- Grossiord C, Buckley T N, Cernusak L A, Novick K A, Poulter B, Siegwolf R T W, Sperry J S and McDowell N G 2020 Plant responses to rising vapor pressure deficit *New Phytol.* **226** 1550–66
- Hagmann R K *et al* 2021 Evidence for widespread changes in the structure, composition, and fire regimes of western North American forests *Ecol. Appl.* **31** e02431
- Haikerwal A, Akram M, Sim M R, Meyer M, Abramson M J and Dennekamp M 2016 Fine particulate matter (PM_{2.5}) exposure during a prolonged wildfire period and emergency department visits for asthma *Respirology* **21** 88–94
- Hall R J *et al* 2020 Generating annual estimates of forest fire disturbance in Canada: the national burned area composite *Int. J. Wildland Fire* **29** 878–91
- Hanes C C, Wang X, Jain P, Parisien M-A, Little J M and Flannigan M D 2019 Fire-regime changes in Canada over the last half century *Can. J. For. Res.* **49** 256–69
- Hansen J, Ruedy R, Sato M and Lo K 2010 Global surface temperature change *Rev. Geophys.* **48** 1–29
- Hawkins E and Sutton R 2009 The potential to narrow uncertainty in regional climate predictions *Bull. Amer. Meteor. Soc.* **90** 1095–108
- Heft-Neal S, Driscoll A, Yang W, Shaw G and Burke M 2022 Associations between wildfire smoke exposure during pregnancy and risk of preterm birth in California *Environ. Res.* **203** 111872
- IPCC 2022 Summary for policymakers *Climate Change 2022: Impacts, Adaptation and Vulnerability. Contribution of Working Group II to the Sixth Assessment Report of the Intergovernmental Panel on Climate Change* (Cambridge: Cambridge University Press) pp 3–33
- James R, Washington R, Schleussner C-F, Rogelj J and Conway D 2017 Characterizing half-a-degree difference: a review of methods for identifying regional climate responses to global warming targets *WIREs Clim. Change* **8** e457
- Jolly W M, Cochrane M A, Freeborn P H, Holden Z A, Brown T J, Williamson G J and Bowman D M J S 2015 Climate-induced variations in global wildfire danger from 1979 to 2013 *Nat. Commun.* **6** 7537
- Juang C S, Williams A P, Abatzoglou J T, Balch J K, Hurteau M D and Moritz M A 2022 Rapid growth of large forest fires drives the exponential response of annual forest-fire area to aridity in the Western United States *Geophys. Res. Lett.* **49** e2021GL097131
- Kirchmeier-Young M C, Zwiers F W, Gillett N P and Cannon A J 2017 Attributing extreme fire risk in Western Canada to human emissions *Clim. Change* **144** 365–79
- Lee J-Y *et al* 2021 Future global climate: scenario-based projections and nearterm information *Climate Change 2021: The Physical Science Basis. Contribution of Working Group I to the Sixth Assessment Report of the Intergovernmental Panel on Climate Change* ed V Masson-Delmotte *et al* (Cambridge: Cambridge University Press) pp 553–672 (available at: www.ipcc.ch/report/ar6/wg1/downloads/report/IPCC_AR6_WGI_Chapter04.pdf)
- Licker R, Ekwurzel B, Doney S C, Cooley S R, Lima I D, Heede R and Frumhoff P C 2019 Attributing ocean acidification to major carbon producers *Environ. Res. Lett.* **14** 124060
- Liu Z, Deng Z, Davis S J, Giron C and Ciais P 2022 Monitoring global carbon emissions in 2021 *Nat. Rev. Earth. Environ.* **3** 217–9
- Medellín-Azuara J, Escrivá-Bou A, Rodríguez-Flores J M, Cole S A, Abatzoglou J T, Viers J H, Santos N and Summer D A 2022 *Economic Impacts of the 2020–22 Drought on California Agriculture* (Merced: University of California, Merced) (available at: https://wsn.ucmerced.edu/wp-content/uploads/2022/11/Economic_Impact_CA_Drought_V01.pdf)
- Millar R J, Nicholls Z R, Friedlingstein P and Allen M R 2017 A modified impulse-response representation of the global near-surface air temperature and atmospheric concentration response to carbon dioxide emissions *Atmos. Chem. Phys.* **17** 7213–28
- Mitchell T D 2003 Pattern scaling: an examination of the accuracy of the technique for describing future climates *Clim. Change* **60** 217–42
- National Interagency Fire Center 2022 *Federal Firefighting Costs (Suppression Only)* (available at: www.nifc.gov/sites/default/files/document-media/suppcosts.pdf)
- Natural Resources Canada 2021 Cost of wildland fire protection (available at: www.nrcan.gc.ca/climate-change/impacts-adaptations/climate-change-impacts-forests/forest-change-indicators/cost-fire-protection/17783)
- Parks S A and Abatzoglou J T 2020 Warmer and drier fire seasons contribute to increases in area burned at high severity in western US forests from 1985 to 2017 *Geophys. Res. Lett.* **47** e2020GL089858
- Perrone D and Jasechko S 2017 Dry groundwater wells in the western United States *Environ. Res. Lett.* **12** 104002
- Scholl A E and Taylor A H 2010 Fire regimes, forest change, and self-organization in an old-growth mixed-conifer forest, Yosemite National Park, USA *Ecol. Appl.* **20** 362–80
- Seager R, Hooks A, Williams A P, Cook B, Nakamura J and Henderson N 2015 Climatology, variability, and trends in the U.S. vapor pressure deficit, an important fire-related meteorological quantity *J. Appl. Meteorol. Climatol.* **54** 1121–41
- Stevens-Rumann C S, Kemp K B, Higuera P E, Harvey B J, Rother M T, Donato D C, Morgan P and Veblen T T 2018

- Evidence for declining forest resilience to wildfires under climate change *Ecol. Lett.* **21** 243–52
- Stokstad E 2020 Droughts exposed California's thirst for groundwater. Now, the state hopes to refill its aquifers *Science* | AAAS (available at: www.sciencemag.org/news/2020/04/droughts-exposed-california-s-thirst-groundwater-now-state-hopes-refill-its-aquifers)
- Supran G and Oreskes N 2017 Assessing ExxonMobil's climate change communications (1977–2014) *Environ. Res. Lett.* **12** 084019
- Supran G and Oreskes N 2021 Rhetoric and frame analysis of ExxonMobil's climate change communications: one Earth *One Earth* **4** 696–719
- Wang D et al 2021 Economic footprint of California wildfires in 2018 *Nat. Sustain.* **4** 252–60
- Westerling A L 2016 Increasing western US forest wildfire activity: sensitivity to changes in the timing of spring *Philos. Trans. R. Soc. B* **371** 20150178
- Westerling A L, Hidalgo H G, Cayan D R and Swetnam T W 2006 Warming and earlier spring increase western U.S. forest wildfire activity *Science* **313** 940–3
- Whitman E, Parks S A, Holsinger L M and Parisien M-A 2022 Climate-induced fire regime amplification in Alberta, Canada *Environ. Res. Lett.* **17** 055003
- Williams A P et al 2014 Correlations between components of the water balance and burned area reveal new insights for predicting forest fire area in the southwest United States *Int. J. Wildland Fire* **24** 14–26
- Williams A P, Abatzoglou J T, Gershunov A, Guzman-Morales J, Bishop D A, Balch J K and Lettenmaier D P 2019 Observed impacts of anthropogenic climate change on wildfire in California *Earth's Future* **7** 892–910
- Williams A P, Cook B I and Smerdon J E 2022 Rapid intensification of the emerging southwestern North American megadrought in 2020–2021 *Nat. Clim. Change* **12** 232–4
- Zhuang Y, Fu R, Santer B D, Dickinson R E and Hall A 2021 Quantifying contributions of natural variability and anthropogenic forcings on increased fire weather risk over the western United States *Proc. Natl Acad. Sci.* **118** e2111875118